

Ground-state fidelity in the BCS-BEC crossover

Ayan Khan and Pierbiagio Pieri

Dipartimento di Fisica, Università di Camerino, I-62032 Camerino, Italy

(Dated: October 29, 2018)

The ground-state fidelity has been introduced recently as a tool to investigate quantum phase transitions. Here, we apply this concept in the context of a crossover problem. Specifically, we calculate the fidelity susceptibility for the BCS ground-state wave function, when the intensity of the fermionic attraction is varied from weak to strong in an interacting Fermi system, through the BCS-BEC crossover. Results are presented for contact and finite-range attractive potentials and for both continuum and lattice models. We conclude that the fidelity susceptibility can be useful also in the context of crossover problems.

PACS numbers: 03.67.-a, 05.70.Jk, 03.75.Lm

I. INTRODUCTION

A quantum phase transition is an abrupt change of the ground state of a many-body system when a controlling parameter λ of the Hamiltonian crosses a critical value λ_c . It is then quite natural to expect¹ that the overlap $F(\lambda + \delta\lambda, \lambda) \equiv |\langle \Psi(\lambda + \delta\lambda) | \Psi(\lambda) \rangle|$ between the ground states corresponding to two slightly different values of the parameter λ , should manifest an abrupt drop when the small variation $\delta\lambda$ crosses λ_c . Such overlap, which has been named “ground-state fidelity” in the literature, should thus provide a tracer of a quantum phase transition. An appealing feature of the ground-state fidelity is that it does not rely on the explicit knowledge, or even the very existence, of an order parameter associated with the quantum phase transition.

The ground-state fidelity approach to quantum phase-transitions has been tested in a variety of models^{1,2,3,4,5,6,7,8,9,10,11,12,13,14,15,16,17,18}, and has been found to be quite effective in signalling the presence of a quantum phase transition. In particular, even phase transitions which are not associated directly with a local order parameter, like transitions topological in nature or of the Beresinskii-Kosterlitz-Thouless type have been found to be detectable by the ground-state fidelity (or derived quantities like the fidelity susceptibility)^{3,9,13,19}. [Some phase transitions of high order in terms of the controlling parameter λ have been found, however, to escape the analysis based on the ground-state fidelity⁵.]

In the present paper we make a step further in the study of the potentialities of the ground-state fidelity, by analyzing its applicability beyond the domain for which it was originally conceived. We consider specifically a *crossover* problem, that is, a many-body system for which a substantial change in the nature of its ground state occurs over a *finite* range of the controlling parameter λ , rather than abruptly at a critical value λ_c . On physical grounds, we expect that the sudden drop of the ground-state fidelity at a critical value λ_c should in this case be replaced by a minimum, located in the region of λ where the ground state is changing more rapidly, namely, in the crossover region. In terms of the fidelity susceptibility (defined shortly below), the divergence at

a critical point should correspondingly be replaced by a peak, whose width should be associated with the width of the crossover region.

To test the above ideas we consider specifically the BCS-BEC crossover, namely, the evolution of the ground state of a fermionic system in the presence of an attractive potential which is progressively increased in its strength. This evolution, first studied in Refs. 20,21,22, has been studied then quite extensively, firstly in connection with the physics of high-temperature cuprate superconductors^{23,24,25,26,27,28}, and more recently with ultracold Fermi atoms, where this crossover has been realized experimentally^{29,30,31,32,33,34}. Several models supporting this crossover will be analyzed, both in continuum and discrete space. Such a systematic analysis will allow us to draw conclusions of sufficient generality, which we believe to be applicable also to other crossover problems.

The paper is organized as follows. In Sec. II we introduce the fidelity susceptibility and derive its expression for the BCS wave-function. This quantity is calculated explicitly in Sec. III for the BCS-BEC crossover in continuum models. We consider specifically the three-dimensional contact and Nozierés-Schmitt-Rink potentials, and compare the information extracted from the fidelity susceptibility with what is already known in the literature for the BCS-BEC crossover in these models. A similar analysis is presented in Sec. IV for the attractive Hubbard model (in both two and three dimensions). Section V gives our conclusions.

II. THE FIDELITY SUSCEPTIBILITY FOR THE BCS WAVE FUNCTION

The ground-state fidelity $F(\lambda + \delta\lambda, \lambda)$ depends, by its definition, on both the controlling parameter λ and its variation, $\delta\lambda$. The somewhat artificial dependence on the actual value of the parameter $\delta\lambda$ can be eliminated by considering the limiting expression for the ground-state

fidelity when $\delta\lambda$ approaches zero. For small $\delta\lambda$:

$$\begin{aligned} F(\lambda + \delta\lambda, \lambda)^2 &= \left[\langle \Psi(\lambda) | + \delta\lambda \frac{\partial \langle \Psi(\lambda) |}{\partial \lambda} \right. \\ &\quad \left. + \frac{(\delta\lambda)^2}{2} \frac{\partial^2 \langle \Psi(\lambda) |}{\partial \lambda^2} \right] \cdot | \Psi(\lambda) \rangle \quad (1) \\ &= 1 - \frac{(\delta\lambda)^2}{2} \frac{\partial \langle \Psi(\lambda) |}{\partial \lambda} \cdot \frac{\partial | \Psi(\lambda) \rangle}{\partial \lambda}, \quad (2) \end{aligned}$$

where the state $|\Psi(\lambda)\rangle$ is assumed to be real and normalized. A sudden drop of the ground-state fidelity at the critical point will then correspond to a divergence of the *fidelity susceptibility*^{2,3}:

$$\chi(\lambda) \equiv -\frac{1}{\Omega} \lim_{\delta\lambda \rightarrow 0} \frac{4 \ln F(\lambda + \delta\lambda, \lambda)}{(\delta\lambda)^2} \quad (3)$$

$$= \frac{1}{\Omega} \frac{\partial \langle \Psi(\lambda) |}{\partial \lambda} \cdot \frac{\partial | \Psi(\lambda) \rangle}{\partial \lambda}. \quad (4)$$

Note that, in order to deal with a meaningful quantity in the thermodynamic limit, the expressions on the right-hand side of Eqs. (3) and (4) in the definition of the fidelity susceptibility have been divided by the system volume Ω . For a sufficiently large system, one has in fact $\ln F(\lambda, \lambda') \propto \Omega$. Indeed, barring the case when a correlation length ξ diverges (i.e. when λ or λ' sit exactly at a critical point), the system can be thought as a collection (tensor product) of many identical subsystems of volume L^D (with $L \gg \xi$ and where D is the spatial dimension). The overlap between two different ground states $|\Psi(\lambda)\rangle$ and $|\Psi(\lambda')\rangle$ will be then the product of the overlaps in each individual subsystem, yielding $F(\lambda, \lambda') \propto f(\lambda, \lambda')^{N_s}$, where $f(\lambda, \lambda')$ is the overlap in each subsystem and $N_s = \Omega/(L^D)$ is the total number of subsystems. This implies then $\ln F(\lambda, \lambda') \propto \Omega$ except when λ or λ' are exactly at a critical point⁵.

In this paper, we are interested in calculating the fidelity susceptibility $\chi(\lambda)$ across the BCS-BEC crossover. Previous studies^{21,22,35} have shown that the BCS wave-function provides a reasonably good approximation for the ground-state wave-function over the whole BCS-BEC crossover, from the weak-coupling limit of highly overlapping Cooper pairs to the strong-coupling limit of tightly bound dilute composite bosons.

We will thus calculate $\chi(\lambda)$ for the BCS wave-function:

$$|\Psi(\lambda)\rangle = \prod_{\mathbf{k}} [u_{\mathbf{k}}(\lambda) + v_{\mathbf{k}}(\lambda) c_{\mathbf{k}\uparrow}^\dagger c_{-\mathbf{k}\downarrow}^\dagger] |0\rangle. \quad (5)$$

Here, $c_{\mathbf{k}\sigma}^\dagger$ creates a fermion in the single-particle state of wave-vector \mathbf{k} , spin σ and energy $\epsilon_{\mathbf{k}}$, $u_{\mathbf{k}}$ and $v_{\mathbf{k}}$ are the usual BCS coherence factor $v_{\mathbf{k}}^2 = 1 - u_{\mathbf{k}}^2 = (1 - \xi_{\mathbf{k}}/E_{\mathbf{k}})/2$, with $\xi_{\mathbf{k}} = \epsilon_{\mathbf{k}} - \mu$, $E_{\mathbf{k}} = \sqrt{\xi_{\mathbf{k}}^2 + \Delta_{\mathbf{k}}^2}$, where μ is the chemical potential and $\Delta_{\mathbf{k}}$ the BCS gap function. The parameter λ in Eq.(5) stands generically for the appropriate coupling strength of the attractive interaction $V_\lambda(k, k')$ which is driving the BCS-BEC crossover. The dependence of $u_{\mathbf{k}}$ and $v_{\mathbf{k}}$ on λ in Eq.(5) is determined by the

gap function $\Delta_{\mathbf{k}}$ and chemical potential μ , which depend on λ through the gap and particle number equations:

$$\Delta_{\mathbf{k}} = - \int \frac{d\mathbf{k}'}{(2\pi)^D} V_\lambda(\mathbf{k}, \mathbf{k}') \frac{\Delta_{\mathbf{k}'}}{2E_{\mathbf{k}'}} \quad (6)$$

$$n = \int \frac{d\mathbf{k}}{(2\pi)^D} 2 v_{\mathbf{k}}^2 \quad (7)$$

where n is the particle number density.

When the BCS wave function is inserted in Eq. (4) for $\chi(\lambda)$ one obtains:

$$\chi(\lambda) = \int \frac{d\mathbf{k}}{(2\pi)^D} \left[\left(\frac{du_{\mathbf{k}}}{d\lambda} \right)^2 + \left(\frac{dv_{\mathbf{k}}}{d\lambda} \right)^2 \right] \quad (8)$$

which, after some manipulations, can be written

$$\chi(\lambda) = \int \frac{d\mathbf{k}}{(2\pi)^D} \frac{1}{4E_{\mathbf{k}}^4} \left[\Delta_{\mathbf{k}} \frac{d\mu}{d\lambda} + \xi_{\mathbf{k}} \frac{d\Delta_{\mathbf{k}}}{d\lambda} \right]^2. \quad (9)$$

In the next two sections we will analyze the behaviour of the fidelity susceptibility for several type of attractive interaction $V_\lambda(k, k')$, by solving the coupled Eqs. (6) and (7) and by calculating then $\chi(\lambda)$ as determined by Eq. (9). Section III will consider continuum models, while section IV will deal with a lattice model (the attractive Hubbard model). In that case the integration over k in Eqs. (6),(7) and (9) will be limited to the first Brillouin zone.

III. CONTINUUM MODELS: CONTACT AND FINITE-RANGE POTENTIALS

The simplest model Hamiltonian for the BCS-BEC crossover describes a system of fermions of mass m in continuum space, mutually interacting via a contact (δ -like) interaction:

$$\begin{aligned} H &= \sum_{\sigma} \int d\mathbf{r} \psi_{\sigma}^\dagger(\mathbf{r}) \frac{-\nabla^2}{2m} \psi_{\sigma}(\mathbf{r}) \\ &\quad + g \int d\mathbf{r} \psi_{\uparrow}^\dagger(\mathbf{r}) \psi_{\downarrow}^\dagger(\mathbf{r}) \psi_{\downarrow}(\mathbf{r}) \psi_{\uparrow}(\mathbf{r}). \quad (10) \end{aligned}$$

The Hamiltonian (10) leads to ultraviolet divergencies, as it can be seen in the gap equation (6) when both the gap function and the interaction do not depend on wave vector (as it occurs for a contact potential). These divergencies are, however, eliminated by expressing physical quantities in terms of the two-body scattering length a_F rather than the bare coupling g .

The above Hamiltonian (with the appropriate ultraviolet regularization) has been studied quite extensively in the context of the BCS-BEC crossover, especially after the advent of experiments with ultracold Fermi atoms in the presence of a Fano-Feshbach resonance^{29,30,31,32,33,34}. For these systems the Hamiltonian (10) can in fact be derived from first principles³⁶, as the effective Hamiltonian

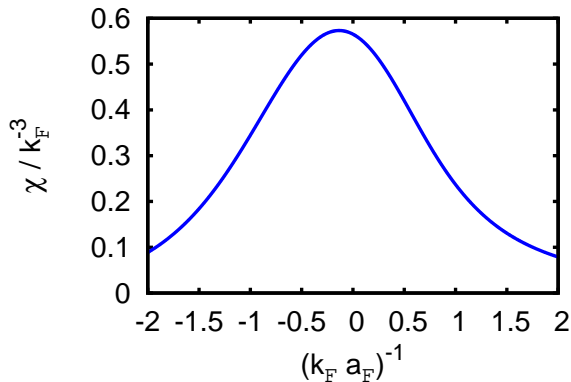


FIG. 1: Fidelity susceptibility (in units of k_F^{-3}) for the three-dimensional contact potential as a function of the dimensionless coupling strength $(k_F a_F)^{-1}$.

describing the physics of the relevant degrees of freedom close to the Fano-Feshbach resonance.

For a three dimensional contact potential the gap equation (6), when expressed in terms of the scattering length a_F reads:

$$-\frac{m}{4\pi a_F} = \int \frac{d\mathbf{k}}{(2\pi)^3} \left(\frac{1}{2E_k} - \frac{m}{k^2} \right). \quad (11)$$

The coupled Eqs. (11) and (7) determine the gap Δ and chemical potential μ in terms of the scattering length a_F or, better, of the dimensionless coupling parameter $(k_F a_F)^{-1}$, which is normally used as the coupling strength parameter for the 3D contact potential (here $k_F \equiv (3\pi^2 n)^{1/3}$, such that the scattering length a_F is compared with the average interparticle spacing k_F^{-1}).

In terms of this parameter the BCS and BEC limits correspond in principle to the conditions $(k_F a_F)^{-1} \ll -1$ and $(k_F a_F)^{-1} \gg 1$, respectively. Previous studies^{37,38,39,40,41} have shown, however, that the crossover between the above two different physical situations is limited in practice to the rather narrow region $-1 \lesssim (k_F a_F)^{-1} \lesssim 1$.

We have calculated the fidelity susceptibility (9), where as a controlling parameter λ we have taken the dimensionless coupling strength (i.e. $\lambda = (k_F a_F)^{-1}$), by solving the coupled Eqs. (11) and (7) (which can be suitably expressed in terms of elliptic integrals³⁹) to determine $\Delta(\lambda)$, $\mu(\lambda)$ and then $\chi(\lambda)$ through the BCS-BEC crossover. The resulting fidelity susceptibility $\chi((k_F a_F)^{-1})$ is presented in Fig. 1.

The fidelity susceptibility presents a rather symmetric peak, which is located in the middle of the crossover region (specifically, the peak position corresponds to $(k_F a_F)^{-1} \simeq -0.14$) and whose half-height width marks precisely the borders of the crossover region $-1 \lesssim (k_F a_F)^{-1} \lesssim 1$ mentioned above. Note that the size of

the crossover region for the three-dimensional contact potential was determined in previous studies by calculating specific physical quantities, like e.g. the chemical potential, the BCS gap, or the superfluid critical temperature and by comparing their numerical values with analytic expressions valid in the BCS and BEC limits, respectively. This empirical way of defining the range of the crossover region, even though physically sound, could be criticized because of some degree of arbitrariness in choosing the physical quantity to look after, or the quantitative criterion to conclude that a specific asymptotic (BEC or BCS) expression has been effectively reached.

The plot of the fidelity susceptibility $\chi((k_F a_F)^{-1})$ of Fig. 1 provides a somewhat more “intrinsic” criterion to locate the position and width of the crossover region, since it is not based on a specific physical quantity but on the measure of the rapidity of change of the ground-state wave-function through the crossover. The agreement between the position and width of the crossover region, as determined by the fidelity susceptibility, with previous results obtained with more empirical criteria to characterize the crossover region corroborates these previous results while proving, at the same time, the utility of the ground-state fidelity for studying also crossover problems.

We pass now to consider a finite-range potential. Specifically, we consider the separable potential introduced by Nozières and Schmitt-Rink²² (NSR):

$$V(k, k') = \frac{-V}{\sqrt{1 + (k/k_0)^2} \sqrt{1 + (k'/k_0)^2}} \quad (12)$$

where k_0 sets the range of the potential in momentum space. The finite range of the NSR potential allows for the occurrence of the density induced BCS-BEC crossover⁴² which is instead not possible in the case of a contact potential.

We have calculated the fidelity susceptibility for the NSR potential (with $\lambda = V$) for various values of the particle density (which can be parametrized by the ratio between k_F and the momentum range of the potential k_0). For each density, our calculated $\chi(V)$ are peaked at a value $V = V_p$ whose position indicates where the rate of change of the BCS wave-function with respect to V is maximal. As already argued above, the value V_p should thus be located in the crossover region.

Fig. 2 compares the peak position V_p extracted from the fidelity susceptibility for several values of k_F/k_0 (full line) with the curves defined by the conditions $k_F \xi_{\text{pair}} = 2\pi$ (dashed line) and $k_F \xi_{\text{pair}} = 1/\pi$ (dash-dotted line), obtained previously in Ref. 42 and introduced there to characterize the width of the crossover region (thus defining a sort of “phase diagram” for the BCS-BEC crossover). In particular, ξ_{pair} represents the pair correlation length, as defined in Ref. 26, and provides an estimate of the Cooper pair radius. The BCS region is characterized by large overlapping Cooper pairs (such that $k_F \xi_{\text{pair}} \gg 1$) while for the BEC region, with small nonoverlapping boson, $k_F \xi_{\text{pair}} \ll 1$. The two values

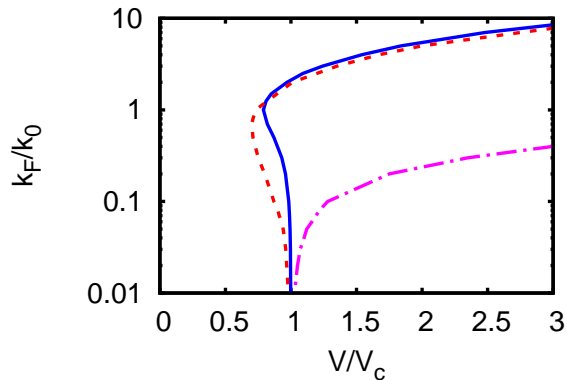


FIG. 2: Crossover “phase diagram” for the three-dimensional NSR potential. The full curve was obtained by determining the position of the peak in the fidelity susceptibility $\chi(V)$ at given values of the parameter k_F/k_0 . The dashed and dash-dotted curves correspond to the BCS and BEC borders of the crossover region, respectively, as determined in Ref. 42. The potential strength V is in units of the critical potential strength $V_c = 4\pi/(mk_0)$.

$(2\pi, 1/\pi)$ of the parameter $k_F\xi_{\text{pair}}$ were taken in Ref. 26 as representative of the BCS and BEC borders of the crossover region, essentially on the basis of the behaviour of the chemical potential as a function of the parameter $k_F\xi_{\text{pair}}$ itself.

We can see from Fig. 2 that the curve corresponding to the peak position V_p extracted from the fidelity susceptibility lies as expected in the middle of the crossover region for $k_F/k_0 \lesssim 1$. For higher densities it approaches instead the BCS edge of this region. This may be due to the fact that at these densities and for $k_F\xi_{\text{pair}}$ of order unity (as in the middle of the crossover region), the range of the attractive potential becomes larger than the Cooper pair size. This favours the clustering of pairs (and eventually leads to an instability for sufficiently strong attraction, because of dominant pair-pair attractive interaction^{24,43,44}). The pair correlation length will thus be increasingly influenced by inter-pair correlations rather than by intra-pair correlations. This implies that at high densities ξ_{pair} tend to overestimate the actual radius of a Cooper pair. At high densities the curve obtained from the peak position in the fidelity susceptibility, which is not based on ξ_{pair} and is thus not influenced by this effect, is thus arguably a better indicator for the position of the crossover region than what is obtained from the calculation of $k_F\xi_{\text{pair}}$ itself.

Note finally the merging of the three curves into the single point $V = V_c$ for vanishing k_F/k_0 . This is expected on physical grounds since in the two-body problem a qualitative change in the ground state (from a delocalized to a localized wave function) occurs precisely at $V = V_c$. It is indeed easy to verify that the fidelity

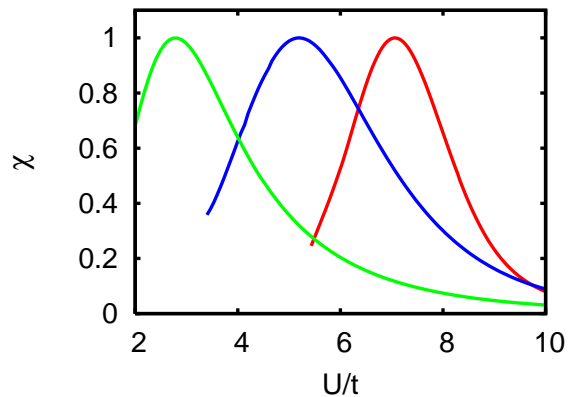


FIG. 3: Fidelity susceptibility (normalized for convenience to the peak value) for the three-dimensional attractive Hubbard model at filling values $n = 0.25, 0.05, 0.005$ from left to right.

susceptibility calculated over the two body wave function diverges at $V = V_c$. At low densities, the fidelity susceptibility approaches the two-body behaviour and is thus peaked around V_c . More generally, when the interparticle distance gets larger than the range of the potential the universal behaviour described by the contact potential is recovered. Since, as we have seen above, for this potential the crossover occurs in the region $|k_F a_F| \gtrsim 1$, it is then clear that when k_F is vanishing the scattering length a_F is bound to diverge in order to keep the product $|k_F a_F| \gtrsim 1$, thus pinning the crossover region close to $V = V_c$ where the scattering length diverges.

IV. ATTRACTIVE HUBBARD MODEL

We analyze finally the fidelity susceptibility calculated over the BCS wave function for the attractive Hubbard model with nearest-neighbour hopping:

$$H = -t \sum_{\langle i,j \rangle \sigma} c_{i\sigma}^\dagger c_{j\sigma} - U \sum_i c_{i\uparrow}^\dagger c_{i\uparrow} c_{i\downarrow}^\dagger c_{i\downarrow} \quad (13)$$

where $\langle i, j \rangle$ indicates a sum over nearest-neighbor pairs and $c_{i\sigma}^\dagger$ creates one electron with spin σ in the Wannier state centered around the lattice site i . For an s -wave gap, which does not depend on \mathbf{k} , the wave vector sums in the gap and particle number Eqs. (6),(7) and in Eq. (9) for the fidelity susceptibility are more efficiently calculated by converting them into integrals over the energy and by using the density of states appropriate for the lattice kinetic energy dispersion.

The resulting fidelity susceptibility for the three-dimensional attractive Hubbard model is shown in Fig. 3, at three different values of the filling factor n (particle number per lattice site). For decreasing filling, the peak in the fidelity susceptibility progressively narrows

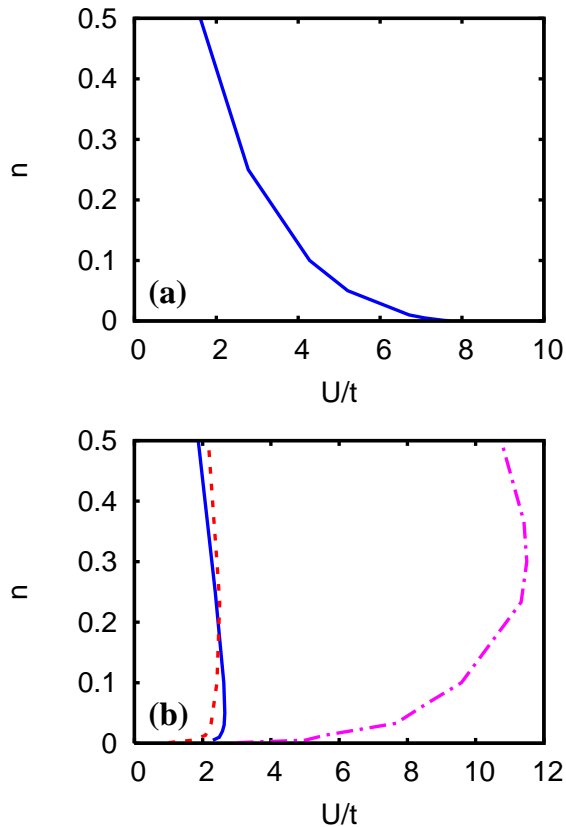


FIG. 4: Attractive Hubbard model: position of the peak in the fidelity susceptibility $\chi(U)$ in the plane $(U/t, n)$ in three (a) and two (b) dimension. In two dimensions the curves corresponding to the BCS and BEC borders of the crossover region as determined in Ref. 42 are also reported for comparison (dashed and dash-dotted curves, respectively).

in width, while its position approaches the critical value ($U_c \simeq 7.9t$) above which a bound state appears in the two-body problem. The width of the crossover region as extracted from the half-height width in the fidelity susceptibility thus shrinks for decreasing density. This overall behaviour of the fidelity susceptibility suggests a progressive approaching of the BCS-BEC crossover towards a quantum phase transition for decreasing density. It is in fact the presence of a finite density in the many-body problem which smears out over a finite coupling range the sudden change occurring at U_c in the two-body problem. In addition, dynamical mean field calculations^{45,46} have shown the occurrence of a quantum phase transition between a Fermi liquid state and a paired state when superconductivity is artificially suppressed in the attractive Hubbard model. This transition, which also approaches the critical value U_c for the two-body problem for vanishing density, is transformed into a crossover when superconducting correlations are restored (in the very same way the metal-insulator transition is transformed into a

crossover within the antiferromagnetic state in the half-filled repulsive Hubbard model). The behaviour of the fidelity susceptibility at low densities can thus be interpreted as the remnant, within the superconducting state, of such underlying quantum phase transition in the normal state.

Fig. 4 compares finally the peak position in the fidelity susceptibility $\chi(U)$ in three and two dimensions (full lines in panel (a) and (b), respectively). In two dimensions the curves corresponding to the conditions $k_F \xi_{\text{pair}} = 2\pi$ (dashed line) and $k_F \xi_{\text{pair}} = 1/\pi$ (dash-dotted line), obtained previously in Ref. 42 are also reported (the three dimensional Hubbard model was instead not considered in Ref. 42). From Fig. 4 (b) we can see that at low filling the peak position in $\chi(U)$ lies in the middle of the crossover region, while at higher filling it bends towards the BCS border of the crossover region, similarly to what found for the three-dimensional NSR continuum potential. We think that also in this case the increasing importance of inter-pair correlations at higher densities explains the relative behaviour of the two curves in this regime. Note, in this respect, that for the Hubbard model it is the lattice spacing to provide the additional length scale relevant at high densities, playing the same role as the finite range of the interaction for the NSR potential.

Note, finally, that in two dimensions the three curves reported in Fig. 4 (b) tend to the “critical” value for the two-body problem ($U = 0$) only at extremely low fillings (recall that in two dimensions, a bound state occurs in the two-body problem as soon as the attraction U is switched on), while in three-dimensions (Fig. 4 (a)) the peak position in the fidelity approaches the two-body critical value $U_c \simeq 7.9t$ more progressively. The behaviour of the three curves at low fillings can be explained by recalling that in two dimensions the binding energy of the two body problem $\epsilon_0 \propto \exp(-t/U)$, while at low densities the Fermi energy relative to the bottom of the band is proportional to the filling ($\epsilon_F \propto n$), such that when ϵ_0 and ϵ_F are of the same order (as it occurs for a crossover curve) one has $n \propto \exp(-t/U)$. This explains the rapid collapsing to zero of the three curves when $U/t \lesssim 1$.

V. CONCLUDING REMARKS

In this paper, we have tested the usefulness of the fidelity susceptibility in the context of a crossover problem. We have considered specifically the BCS-BEC crossover, for which the BCS wave function is known to provide a reliable description of the ground-state properties, and calculated the fidelity susceptibility over the BCS wave function for several models exhibiting the above crossover. For the three-dimensional contact potential, we have found that the peak position in the fidelity susceptibility and its width in terms of the dimensionless coupling parameter $(k_F a_F)^{-1}$ are in full agreement with previous knowledge about the position and range of the crossover region in this model (which has been widely studied in

the literature).

For the finite-range NSR potential, the curve resulting from the peak position in the fidelity susceptibility was compared with the crossover “phase diagram” previously obtained in Ref. 42, where the borders of the crossover region were defined on the basis of the value of the ratio ($k_F \xi_{\text{pair}}$) between the pair correlation length and the average interparticle distance. For densities such that the average interparticle distance does not get smaller than the range of the potential, the peak in the fidelity lies as expected in the middle of the crossover region, while for higher densities it tends to approach the BCS border of the crossover, as defined from the value of $k_F \xi_{\text{pair}}$. We have attributed this behaviour to the increasing importance of inter-pair correlations in the extraction of ξ_{pair} from the pair correlation function at high densities.

We have considered finally the attractive Hubbard model. The results in two dimensions compared favorably with the corresponding crossover “phase diagram” of Ref. 42. In three dimensions, we have argued that the fidelity susceptibility is able to evidence within the superconducting state the traces of an underlying quantum phase transition, which has been found previously for the normal state when the superconducting correlations were artificially suppressed^{45,46}.

In summary, from our analysis we conclude that the fidelity susceptibility provides a useful tool to characterize

the width and position of the crossover region in crossover problems, which is especially appealing because of its “intrinsic” and quite general character. The definition and location of the crossover region based on the fidelity susceptibility do not depend, in fact, on specific quantities like, for instance, the pair correlation length ξ_{pair} in the BCS-BEC crossover, which need to be changed when passing from one crossover problem to another one. Even though our analysis was based on the use of an approximate ground state wave function (the BCS trial wave function), the widely tested reliability of such a wave function in the context of the BCS-BEC crossover give us confidence in the robustness of our results. It will be however interesting to consider in future work alternative methods, like e.g. Quantum Monte Carlo or Density Renormalization Group methods, or alternative crossover problems to confirm our main conclusions and place them in a broader context.

Acknowledgments

We thank G.C. Strinati for useful discussions. Partial support by the Italian MUR under contract PRIN-2007 “Ultracold Atoms and Novel Quantum Phases” is acknowledged.

-
- ¹ P. Zanardi and N. Paunković, Phys. Rev. E **74**, 031123 (2006).
- ² W.-L. You, Y.-W. Li, and S.-J. Gu, Phys. Rev. E **76**, 022101 (2007).
- ³ M.-F. Yang, Phys. Rev. B **76**, 180403(R) (2007).
- ⁴ S. Chen, L. Wang, S.-J. Gu, and Y. Wang, Phys. Rev. E **76**, 061108 (2007).
- ⁵ L. Campos Venuti and P. Zanardi, Phys. Rev. Lett. **99**, 095701 (2007).
- ⁶ P. Zanardi, P. Giorda, and M. Cozzini, Phys. Rev. Lett. **99**, 100603 (2007).
- ⁷ M. Cozzini, P. Giorda, and P. Zanardi, Phys. Rev. B **75**, 014439 (2007).
- ⁸ P. Buonsante and A. Vezzani, Phys. Rev. Lett. **98**, 110601 (2007).
- ⁹ A. Hamma, W. Zhang, S. Haas, and D. A. Lidar, Phys. Rev. B **77**, 155111 (2008).
- ¹⁰ Y.-C. Tzeng and M.-F. Yang, Phys. Rev. A **77**, 012311 (2008).
- ¹¹ S. Chen, L. Wang, Y. Hao, and Y. Wang, Phys. Rev. A **77**, 032111 (2008).
- ¹² S.-J. Gu, H.-M. Kwok, W.-Q. Ning, and H.-Q. Lin, Phys. Rev. B **77**, 245109 (2008).
- ¹³ D.F. Abasto, A. Hamma, and P. Zanardi, Phys. Rev. A **78**, 010301(R) (2008).
- ¹⁴ N. Paunković and V.R. Vieira, Phys. Rev. E **77**, 011129 (2008).
- ¹⁵ H.-Q. Zhou, R. Orús, and G. Vidal, Phys. Rev. Lett. **100**, 080601 (2008).
- ¹⁶ J.-H. Zhao, H.-L. Wang, Bo Li, and H.-Q. Zhou, arxiv/0902.1669.
- ¹⁷ H.-L. Wang, J.-H. Zhao, Bo Li, and H.-Q. Zhou, arxiv/0902.1670.
- ¹⁸ E. Eriksson and H. Johannesson, arxiv/0902.3848.
- ¹⁹ S. Garnerone, D. Abasto, S. Haas, and P. Zanardi, Phys. Rev. A **79**, 032302 (2009).
- ²⁰ D. M. Eagles, Phys. Rev. **186**, 456 (1969).
- ²¹ A. J. Leggett, in *Modern Trends in the Theory of Condensed Matter*, edited by A. Pekalski and R. Przystawa, Lecture Notes in Physics, Vol. 115, p. 13 (Springer-Verlag, Berlin, 1980).
- ²² P. Nozières and S. Schmitt-Rink, Jour. Low. Temp. Phys. **59**, 195 (1985).
- ²³ M. Randeria, J.-M. Duan, and L.-Y. Shieh, Phys. Rev. Lett. **62**, 981 (1989).
- ²⁴ R. Micnas, J. Ranninger, and S. Robaszkiewicz, Rev. Mod. Phys. **62**, 113 (1990).
- ²⁵ R. Haussmann, Z. Phys. B **91**, 291 (1993).
- ²⁶ F. Pistolesi and G. C. Strinati, Phys. Rev. B **49**, 6356 (1994).
- ²⁷ S. Stintzing and W. Zwerger, Phys. Rev. B **56**, 9004 (1997).
- ²⁸ B. Jankó, J. Maly, and K. Levin, Phys. Rev. B **56**, R11407 (1997).
- ²⁹ M.W. Zwierlein, C.A. Stan, C.H. Schunck, S.M.F. Raupach, S. Gupta, Z. Hadzibabic, and W. Ketterle, Phys. Rev. Lett. **91**, 250401 (2003).
- ³⁰ C.A. Regal, C. Ticknor, J.L. Bohn, and D.S. Jin, Nature **424**, 47 (2003).
- ³¹ S. Jochim, M. Bartenstein, A. Altmeyer, G. Hendl, S. Riedl, C. Chin, J. Hecker Denschlag, and R. Grimm, Sci-

- ence **302**, 2101 (2003).
- ³² M. Bartenstein, A. Altmeyer, S. Riedl, S. Jochim, C. Chin, J.H. Denschlag, and R. Grimm, Phys. Rev. Lett. **92**, 120401 (2004).
- ³³ M.W. Zwierlein, C.A. Stan, C.H. Schunck, S.M.F. Raupach, A.J. Kerman, and W. Ketterle, Phys. Rev. Lett. **92**, 120403 (2004).
- ³⁴ C.A. Regal, M. Greiner, D.S. Jin, Phys. Rev. Lett. **92**, 040403 (2004).
- ³⁵ A. Perali, P. Pieri, and G.C. Strinati, Phys. Rev. Lett. **93** 100404 (2004).
- ³⁶ S. Simonucci, P. Pieri, and G.C. Strinati, Europhys. Lett. **69**, 713 (2005).
- ³⁷ C.A.R. Sá de Melo, M. Randeria, and J.R. Engelbrecht, Phys. Rev. Lett. **71**, 3202 (1993).
- ³⁸ R. Haussmann, Phys. Rev. B **49**, 12975 (1994).
- ³⁹ M. Marini, F. Pistolesi and G. C. Strinati, Eur. Phys. J. B **1**, 151 (1998).
- ⁴⁰ A. Perali, P. Pieri, G.C. Strinati, and C. Castellani, Phys. Rev. B **66**, 024510 (2002).
- ⁴¹ P. Pieri, L. Pisani, and G.C. Strinati, Phys. Rev. B **70**, 094508 (2004).
- ⁴² N. Andrenacci, A. Perali, P. Pieri and G. C. Strinati, Phys. Rev. B **60**, 12410 (1999).
- ⁴³ F. Pistolesi and G.C. Strinati, Phys. Rev. B **53**, 15168 (1996).
- ⁴⁴ G. Röpke, A. Schnell, P. Schuck, and P. Nozières, Phys. Rev. Lett. **80**, 3177 (1998).
- ⁴⁵ M. Keller, W. Metzner, and U. Schollwöck, Phys. Rev. Lett. **86**, 4612 (2001).
- ⁴⁶ M. Capone, C. Castellani, and M. Grilli, Phys. Rev. Lett. **88**, 126403 (2002).